Biochimica et Biophysica Acta 1827 (2013) 493–501

Contents lists available at SciVerse ScienceDirect

Biochimica et Biophysica Acta

journal homepage: www.elsevier.com/locate/bbabio

Spectroscopic insights into the decreased efficiency of chlorosomes containing bacteriochlorophyll *f*

Gregory S. Orf [a,b], Marcus Tank [c], Kajetan Vogl [c], Dariusz M. Niedzwiedzki [b], Donald A. Bryant [c,d], Robert E. Blankenship [a,b,*]

[a] Departments of Chemistry and Biology, Washington University in St. Louis, St. Louis, MO 63130, USA
[b] Photosynthetic Antenna Research Center (PARC), Washington University in St. Louis, St. Louis, MO 63130, USA
[c] Department of Biochemistry and Molecular Biology, The Pennsylvania State University, University Park, PA 16802, USA
[d] Department of Chemistry and Biochemistry, Montana State University, Bozeman, MT 59717, USA

ARTICLE INFO

Article history:
Received 22 October 2012
Received in revised form 8 January 2013
Accepted 15 January 2013
Available online 24 January 2013

Keywords:
Green sulfur bacteria
Bacteriochlorophyll
Chlorobaculum limnaeum
Chlorosomes
Photosynthesis
Förster Resonance Energy Transfer

ABSTRACT

Chlorosomes are light-harvesting antenna complexes that occur in green photosynthetic bacteria which have only been shown naturally to contain bacteriochlorophyll (BChl) *c*, *d*, or *e* as the principal light-harvesting pigments. BChl *f* has long been thought to be an obvious fourth member of the so-called *Chlorobium* chlorophylls, because it possesses a C-7 formyl group like BChl *e* and lacks a methyl group at C-20 like BChl *d*. In organisms that synthesize BChl *c* or *e*, the *bchU* gene product encodes the enzyme that methylates the C-20 position of these molecules. A *bchU* null mutant of the green sulfur bacterium *Chlorobaculum limnaeum* strain 1677^T, which normally synthesizes BChl *e*, has recently been generated via insertional inactivation, and it produces chlorosomes containing BChl *f* [Vogl et al., 2012]. In this study, chlorosomes containing BChl *f* and monomeric BChl *f* in pyridine were characterized using a variety of spectroscopic techniques, including fluorescence emission and excitation spectroscopy, fluorescence lifetime and quantum yield determinations, and circular dichroism. These spectroscopic measurements, as well as Gaussian simulation of the data, show that chlorosomes containing BChl *f* are less efficient in energy transfer than those with BChl *e*. This can primarily be attributed to the decreased spectral overlap between the oligomeric BChl *f* (energy donor) fluorescence emission and the BChl *a* (energy acceptor) absorption in the chlorosome baseplate. This study allows us to hypothesize that, if they exist in nature, BChl *f*-containing organisms most likely live in rare high-light, anoxic conditions devoid of Chl *a*, *d*, or BChl *e* filtering.

Abstract reference: K. Vogl, M. Tank, G.S. Orf, R.E. Blankenship, D.A. Bryant, Bacteriochlorophyll *f*: properties of chlorosomes containing the "forbidden chlorophyll," *Front. Microbiol.* 3 (2012) 298.

1. Introduction

Chlorosomes are the distinctive light-harvesting antenna complexes of green bacteria, including all phototrophic members of the green sulfur bacterial (GSB) phylum *Chlorobi*, some members of the *Chloroflexi*, and "*Candidatus* Chloracidobacterium thermophilum," the only known chlorophototrophic species of the *Acidobacteria* [1–3]. These large antenna complexes are optimized to operate efficiently at extremely low photon fluxes, which allow these organisms to grow at the lowest irradiance levels recorded for photosynthetic growth [2,4]. In members of the *Chlorobi* and "*Ca*. C. thermophilum," the chlorosome funnels the excitation energy through the baseplate to the Fenna-Matthews-Olson (FMO) protein and then to the reaction center, where the excitation energy is converted to chemical energy.

Chlorosomes are sacs filled with pigments, in which a lipid monolayer envelope, which is interspersed with proteins, surrounds the self-assembled, light-harvesting bacteriochlorophylls (BChls). Single chlorosomes contain between 100,000 and 250,000 BChl *c*, *d*, or *e* molecules, depending on species [5,6]. The self-assembly of the BChl pigments is largely independent of protein influence and several oligomeric structural patterns have been identified [6–11]. Carotenoids and quinones, which aid in light absorption, triplet state quenching, and redox control, are also dispersed throughout the interior of the chlorosome [3,12–15]. The self-assembled BChls transfer excitation energy to the CsmA baseplate, a paracrystalline BChl *a*-protein complex integrated into the lipid monolayer of the chlorosome, which serves as the interface to the FMO protein [16–18].

Bacteriochlorophylls *c*, *d*, and *e* share a common basic structure but differ specifically at their C-7 and C-20 substituents, which

Abbreviations: BChl, bacteriochlorophyll; (B)Chl, bacteriochlorophyll or chlorophyll; Chl, chlorophyll; GSB, green sulfur bacteria; 1-*T*, 1-Transmittance

* Corresponding author at: Campus Box 1137, One Brookings Drive, Departments of Chemistry and Biology, Washington University in St. Louis, St. Louis, MO 63130, USA. Tel.: +1 314 935 7971.
E-mail address: blankenship@wustl.edu (R.E. Blankenship).

0005-2728/$ – see front matter © 2013 Elsevier B.V. All rights reserved.
http://dx.doi.org/10.1016/j.bbabio.2013.01.006

significantly alter their spectral properties. BChls *c* and *d* have a methyl group at the C-7 position, while BChl *e* has a formyl group at this position. BChls *c* and *e* contain a C-20 methyl group, which BChl *d* lacks. There has long been a placeholder name for a fourth member of the *Chlorobium* BChl group, BChl *f*, even though it has not yet been observed naturally [19–21]. The presence of the C-7 formyl group and absence of the C-20 methyl group in BChl *f* represent the last possible combination in the *Chlorobium* BChl pigment family.

Because of the development of a tractable genetic system in the BChl *c*-containing *Chlorobaculum* (*Cba.*) *tepidum*, most of the BChl biosynthesis pathway in this organism has been elucidated [3,22]. The C-20 methyltransferase gene, *bchU*, was identified in 2003 after extensive searching of the genomes of both *Cba. tepidum* and the green non-sulfur bacterium *Chloroflexus aurantiacus*. This gene was subsequently insertionally inactivated in *Cba. tepidum*, which resulted in chlorosomes containing BChl *d* instead of BChl *c* [23]. It was hypothesized that if this gene was also inactivated in a BChl *e*-containing organism, the mutant should produce the long-sought-after BChl *f* [20].

Recently, tractable genetic systems for two BChl *e*-containing strains of *Chlorobaculum limnaeum* were developed, and *bchU* null mutants were constructed that synthesized only BChl *f* [24,25]. Previous predictions concerning the spectral properties of BChl *f* were confirmed. Relative to BChl *e*, the absorption of aggregated BChl *f* was shifted ~15 nm to shorter wavelengths, which results in an absorption maximum centered at ~705 nm at room temperature (Fig. 1). The absorption wavelength maximum of BChl *a* in the CsmA baseplate was unaltered after *bchU* inactivation [24,25].

An important question concerning chlorosomes containing BChl *f* concerns their energy transfer efficiency compared to chlorosomes containing BChl *e*. Initial characterization showed that chlorosomes containing BChl *f* have a lower energy transfer efficiency than the BChl *e*-containing parent strain [24]. A reduced efficiency of energy transfer within chlorosomes would reduce the amount of energy available to the reaction centers and might explain at least in part why BChl *f* has not so far been found in a naturally occurring organism. This manifests itself phenotypically as decreased growth rates at low, physiologically relevant irradiance [24]. Other important questions concern whether the inefficiency has to do with the BChl *f* molecule itself, its organization, or other as yet unknown reasons.

Here, we report a more complete characterization of chlorosomes containing BChl *f*, as well as monomeric BChl *f* dissolved in pyridine and other solvents. Steady-state absorption and fluorescence spectra, circular dichroism, estimates of energy transfer efficiency, BChl *f* monomer fluorescence lifetime and quantum yield measurements, and fitting of the Gaussian simulations of the spectra to Förster Resonance Energy Transfer (FRET) theory strongly suggest that BChl *f* is intrinsically as efficient as a light harvesting molecule as the other BChls in the *Chlorobium* BChl family. However, because the absorption of BChl *f* aggregates is shifted to shorter wavelengths compared to BChl *e* aggregates, the spectral overlap between the BChl *f* donor fluorescence and the BChl *a* acceptor absorption in the baseplate is significantly decreased. This is proposed to be the main reason for the decreased energy transfer efficiency observed in chlorosomes containing BChl *f*. These data also present an opportunity to evaluate the evolutionary consequences of BChl *f* utilization as a major photosynthetic pigment and to describe possible niches in which undiscovered organisms containing BChl *f* may live.

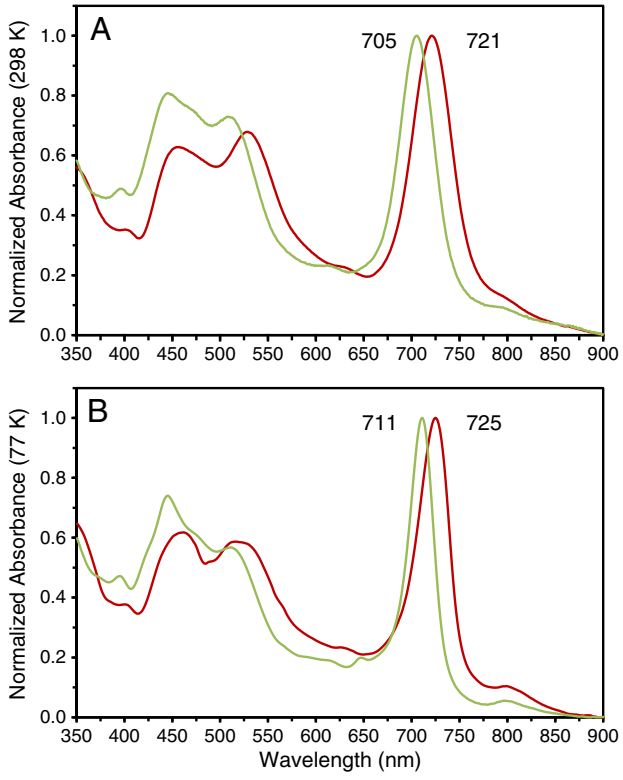

Fig. 1. Absorption spectra of oxidized BChl *e*-containing (red line) and BChl *f*-containing (green line) chlorosomes at room temperature (A) and 77 K (B) recorded in air-saturated buffer. The 77 K spectrum shows the CsmA baseplate is unaltered between the two types of chlorosomes. Adapted from [24].

2. Materials and methods

2.1. Mutagenesis and chlorosome isolation

Growth conditions for wild-type *Cba. limnaeum* WT (BChl *e*-containing), and the construction and growth of a *bchU* mutant strain (BChl *f*-containing) were previously described [24]. *Cba. tepidum* was grown as described previously [26], and cells were used as a source of the BChl *c* that served as a reference for quantum yield measurements.

Whole membranes were prepared from 3–7 day old cell cultures. Cells were centrifuged (7500 ×*g*, 20 min) and were resuspended in 10 mM Tris–HCl buffer, pH 7.5, and were mechanically disrupted using a chilled French press operated at 138 MPa. Large cell debris and unbroken cells were removed by centrifugation (10,000 ×*g* for 20 min). The membranes in the resulting supernatant were concentrated by ultracentrifugation at 220,000 ×*g* for 2 h, redissolved in a minimal volume of 10 mM Tris–HCl buffer, pH 7.5, and stored until needed at 4 °C.

Chlorosomes were isolated as previously described [24]. After purification, the washed and pelleted chlorosomes were resuspended in phosphate buffer (1 to 2 ml) containing 1.0 mM phenylmethylsulfonyl fluoride and 2.0 mM dithiothreitol for long-term storage at 4 °C. Before spectroscopic measurements, the chlorosomes were pelleted again by ultracentrifugation (220,000 ×*g* for 1.5 h) and gently resuspended in 20 mM Tris–HCl buffer, pH 8.0 (1 to 2 mL).

2.2. Absorption and fluorescence measurements

Absorbance and 1-*T* spectra for isolated chlorosomes or whole photosynthetic membranes were measured on a Lambda 950 UV/Vis/NIR spectrophotometer (Perkin Elmer Inc., Waltham, MA) [24]. All fluorescence spectra were measured using a customized PTI fluorometer (Photon Technology International Inc., Birmingham, NJ). The slits in all positions of the fluorometer were adjusted to 1 mm corresponding to a 4 nm spectral bandwidth. Fluorescence was monitored at right angle in respect to excitation. Fluorescence excitation spectra were corrected using a calibrated reference diode. All samples were prepared for fluorescence measurements by diluting with 20 mM Tris–HCl buffer, pH 8.0 to a Q_y absorption value of 0.1. When indicated, samples

were fully reduced by the addition of sodium dithionite to a total concentration of 25 mM with subsequent incubation in the dark for 1 h at 4 °C prior to measurements. Measurements at 77 K were performed by adding glycerol (final concentration, 50%, v/v) to the samples and then cooling with liquid nitrogen in an Optistat DN2 cryostat (Oxford Instruments, Oxfordshire, UK).

For fluorescence emission measurements, isolated chlorosomes were excited at wavelengths corresponding to the two principal components of their absorbance bands at 457 nm and 528 nm for BChl *e* and at 446 nm and 508 nm for BChl *f*. The raw fluorescence emission spectra were scaled in order to correct for the fact that they were recorded with different excitation wavelengths, allowing all spectra to be displayed on the same y-axis for a quantitative comparison. The scaling factor, ($Ordinate_{1\text{-}T\ \text{spectrum for standard at}\ \lambda ex}/Ordinate_{1\text{-}T\ \text{spectrum for sample at}\ \lambda ex}$), corrects for this by adjusting for the different numbers of photons absorbed by each chlorosome sample at their respective excitation wavelengths (λ_{ex}). The 1-*T* spectra were recorded for a solution of BChl *e* chlorosomes of $Abs_{721\ nm} = 0.1$ and for a solution of BChl *f* chlorosomes of $Abs_{705\ nm} = 0.1$. The fluorescence emission spectra for chlorosomes containing BChl *e* from the 457 nm excitation were arbitrarily chosen to be the standard for scaling. Although this scaling is small, it is necessary to reconcile the experimental differences that arise from the use of multiple excitation wavelengths. It should also be noted that the extinction coefficient for BChl *f* is expected to be similar to BChl *e* within ~5%, just as the extinction coefficients of BChl *c* and *d*, which only differ by the C-20 methyl substituent, are quite similar (75 vs. 79 $mM^{-1}\ cm^{-1}$, respectively) [19]. Lastly, for fluorescence excitation spectra, dithionite-reduced whole photosynthetic membranes were used with emission monitored at 830 nm; use of whole membranes allowed for better modeling of the excitation spectrum peak of the CsmA baseplate.

2.3. Pigment extraction from chlorosomes

Purified chlorosomes containing BChl *c* or BChl *f* were pelleted by ultracentrifugation (220,000 ×*g* for 1.5 h) and pigments were extracted with HPLC-grade 7:2 acetone:methanol (100 μL). The pigment solution was transferred to a microcentrifuge tube and centrifuged (13,000 ×*g* for 5 min). The clear, green supernatant was directly injected into an Agilent Series 1100 HPLC system (Aglient Technologies Inc., Santa Clara, CA) equipped with a reverse-phase C-18 column (4.6×250 mm, Agilent Technologies Inc., Santa Clara, CA) regulated at 20 °C. Pigments were eluted with 96:4 methanol:water pumped at a rate of 1 mL min^{-1}. The three main BChl *c* or *f* peaks (corresponding to forms of the pigment differing at the variable C-8^2 or C-12^1 positions) were combined [24].

2.4. Quantum yield measurements of BChl f

For quantum yield measurements, aliquots of purified BChl *c* and BChl *f* were dried under a stream of nitrogen gas and resuspended in 1 mL of degassed pyridine. The samples were transferred to 1 cm square quartz cuvettes with screw tops fitted with rubber septa. Before sealing the cuvettes, the headspace was sparged with nitrogen to eliminate as much oxygen as possible. Degassed pyridine was injected through the rubber septa to adjust the absorbance of the samples at their excitation wavelengths in a series of values between 0.02 and 0.10. While this method did not result in completely anaerobic conditions, absorption spectra were taken to ensure that degradation of the pigments was negligible, as well as to record accurately the absorbance value at the excitation wavelength. Fluorescence emission spectra of BChl *c* and BChl *f* at each absorbance were taken using a 596 nm (BChl *f*) or 618 nm (BChl *c*) excitation beam, measuring emission from 625–950 nm. Fluorescence spectra were integrated to determine quantum yield using BChl *c* ($\Phi_F = 0.27$) as the reference using the method described in [27]. No correction for reabsorption was made because the absorbance values were low enough that the correction values are insignificant. The equation used to calculate quantum yield (Φ_F) [28],

$$\Phi_{F,Analyte} = \Phi_{F,Standard}\left(\frac{Grad_{Analyte}}{Grad_{Standard}}\right)\left(\frac{\eta^2_{Analyte}}{\eta^2_{Standard}}\right) \quad (1)$$

was modified to correct for the fact that the fluorescence spectra for BChl *c* and *f* were not recorded with the same excitation wavelength. The modified equation,

$$\Phi_{F,\ BChl\ f} = \Phi_{F,BChl\ c}\left(\frac{Grad_{BChl\ f}}{Grad_{BChl\ c}}\right)\left(\frac{\eta^2_{BChl\ f}}{\eta^2_{BChl\ c}}\right)\left(\frac{Ordinate_{1-T\ \text{Spectrum at BChl}\ c\ \lambda_{ex}}}{Ordinate_{1-T\ \text{Spectrum at BChl}\ f\ \lambda_{ex}}}\right) \quad (2)$$

corrects for this by adjusting for the different numbers of photons absorbed by each pigment at their respective excitation wavelengths. The 1-*T* spectra were recorded for the BChl *c* solution of $Abs_{618\ nm} = 0.1$ and the BChl *f* solution of $Abs_{596\ nm} = 0.1$. Although this correction is small, it is necessary to reconcile the experimental differences that arise from the use of two different excitation wavelengths. *Grad* refers to the slope of a linear fit of an *x*–*y* scatter plot of integrated fluorescence vs. absorbance and η is the refractive index of the solvent. The η terms cancel because both BChl *c* and *f* were dissolved in the same solvent.

2.5. Fluorescence lifetime measurements of BChl f

Time-resolved fluorescence measurements were carried out using a universal streak camera (Hamamatsu Corp., Bridgewater, NJ) equipped with a cooled N51716-04 streak tube, C5680 blanking unit, Orca2 digital CCD camera, slow speed M5677 unit, C10647 and C1097-05 delay generators and an A6365-01 spectrograph (Bruker Corp., Billerica, MA). Excitation pulses (at 645 nm) were produced by an Inspire 100 ultrafast optical parametric oscillator (OPO) (Radiantis-Spectra-Physics, Barcelona, Spain) pumped with Mai-Tai, an ultrafast Ti:Sapphire laser generating ~90 fs laser pulses at 820 nm with a frequency of 80 MHz. The frequency of the excitation beam was lowered to 8 MHz (125 ns between subsequent excitations) after the OPO using a Pulse Selector 3980 from Spectra-Physics equipped with a 3986 controller. The excitation beam with a power of ~50 mW was focused on the sample in a circular spot of 2 mm diameter, which corresponds to a photon intensity of $\sim 6\times10^{11}$ photons cm^{-2} per pulse.

2.6. Circular dichroism spectroscopy

Circular dichroism (CD) measurements were made on a J-815 spectropolarimeter (JASCO Inc., Easton, MD) detecting in Vis-NIR mode. The sampling resolution was set at 1 nm and the sampling speed was set at 1 nm s^{-1}. Samples were prepared for CD by dilution to a Q_y absorption of 1.0 with 20 mM Tris–HCl buffer, pH 8.0.

2.7. Energy transfer calculations using FRET theory

The fluorescence emission spectra of the dithionite-reduced chlorosomes containing BChl *e* and BChl *f* were simulated by Gaussian functions. To apply a FRET theory treatment and estimate the energy transfer efficiency from main pigment to chlorosome baseplate, we begin with the FRET equations [19]:

$$\phi_{ET} = \frac{1}{1+\left(\frac{R}{R_0}\right)^6} \quad (3)$$

$$where\ R_0^6 = \frac{9Q_0 \ln 10 \kappa^2 J}{128\pi^5 \eta^4 N_A} \quad (4)$$

$$and\ J = \int f_D(\lambda)\epsilon_A(\lambda)\lambda^4 d\lambda \quad (5)$$

ϕ_{ET} refers to the energy transfer efficiency from donor to acceptor ($0 \le \phi_{ET} < 1$), R is the distance between donor and acceptor, Q_0 is the fluorescence quantum yield of the donor, κ^2 is a molecular orientation factor, η is the refractive index of the medium, N_A is the Avogadro's constant, $f_D(\lambda)$ is the fluorescence emission spectrum of the donor molecule, $\in_A(\lambda)$ is the molar extinction plot of the acceptor molecule, and λ is the wavelength. Making the assumption that all parameters except for the spectral overlap integral, J, are equal between the two chlorosomes, Eq. (3) can be simplified to:

$$\phi_{ET} = \frac{1}{1 + \left(\frac{x}{J}\right)} \quad (6)$$

in which x is a constant containing all the variables shared by the two chlorosome systems. The refractive indexes, η, of the two chlorosome systems correspond to the hydrophobic interior of the chlorosomes, which are estimated to be essentially equal, as they contain the same basic components. We also estimated the molar extinction plot of the acceptor molecule, $\in_A$, to be the 1-*T* spectrum of BChl *a* in the baseplate, a Gaussian with an absorption maximum at 789.3 nm and a width of 48.5 nm [29]. By calculating J for both the BChl *e*–BChl *a* pair and the BChl *f*–BChl *a* pair, we can estimate the relationship between efficiencies of the two types of chlorosomes. If, for example, we assume an efficiency level of 0.65 for BChl *e* to BChl *a* transfer (justified in the fluorescence excitation results of Section 3.2), we can calculate x. Using this x and the specific J for BChl *f*, we can calculate an estimated efficiency for BChl *f* to BChl *a* transfer.

3. Results

3.1. Absorption and fluorescence emission spectra

Fig. 2 shows the entire series of GSB pigments in both monomeric form and in their respective chlorosomes, illustrating the different abilities of these organisms to adapt to environmental niches. As shown in Figs. 1 and 2, chlorosomes containing BChl *e* and BChl *f* differ from those containing BChl *c* and *d* because the Soret bands of the BChl oligomers are noticeably split into two components in the absorption spectra at room temperature. The nature of this splitting has been previously explored computationally [30]. It was found that two orthogonally polarized Soret transitions, B_x and B_y, were mostly responsible for the two Soret components. To explore the fluorescence contribution of each of those particular Soret bands in our chlorosome samples experimentally, each peak was individually excited and fluorescence emission spectra were obtained. Because these are Soret bands of the BChl oligomers, we expected that their fluorescence emission would resemble that of BChl oligomers, or through energy transfer, the BChl *a* baseplate. Figs. 3 and 4 correspond to the fluorescence emission spectra obtained from exciting the two Soret band components of chlorosomes containing BChl *e*. The fluorescence emission spectra at both room temperature and 77 K are nearly identical and represent fluorescence emission from both oligomers and the baseplate, which match well with the earlier calculations [30]. It should be noted that the small amount of fluorescence emission at 675 nm observed in Fig. 4A is probably due to a small amount of monomeric BChl *e* present in the chlorosomes, which absorbs at the excitation wavelength for the experiment. The low-temperature fluorescence emission spectra (Figs. 3B and 4B) show a shift to longer wavelengths for all emission maxima. This is

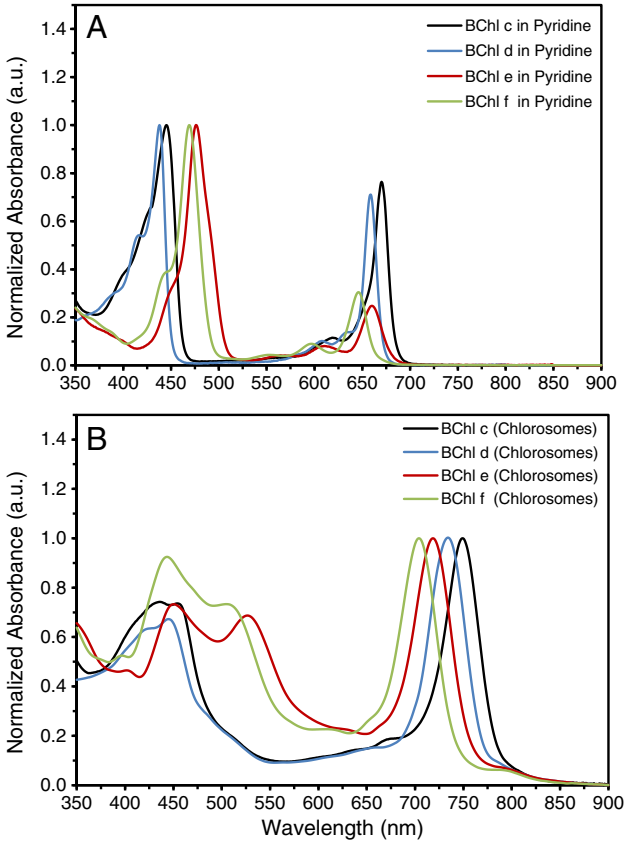

Fig. 2. Absorption spectra of (A) isolated BChls *c*, *d*, *e*, and *f* in pyridine, and (B) whole chlorosomes containing self-assembled BChls *c*, *d*, *e*, and *f*. The data for BChls *c* and *d* come from [29,31], while those for BChls *e* and *f* come from [24] and this study.

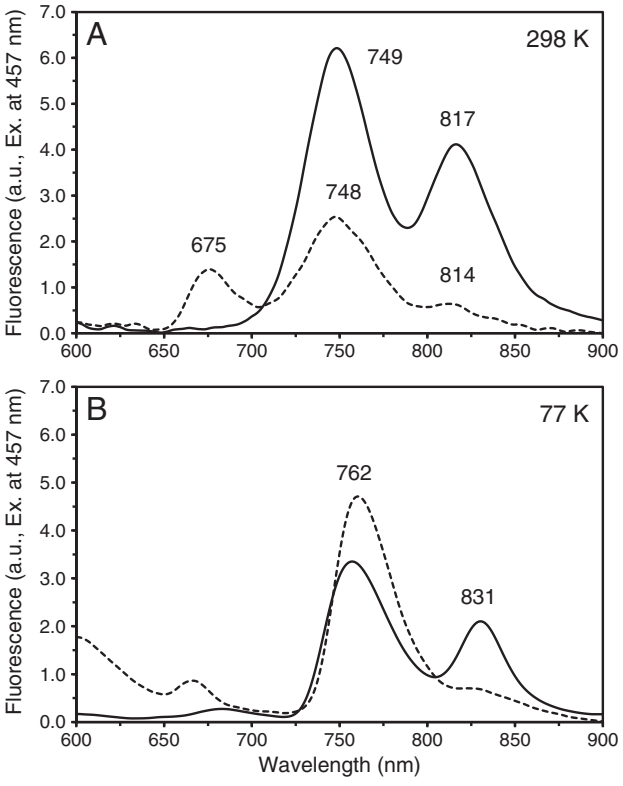

Fig. 3. Fluorescence emission spectra for BChl *e*-containing chlorosomes at room temperature (A) and 77 K (B). The excitation wavelength was into the shorter-wavelength Soret component at 457 nm for each. Spectra of oxidized chlorosomes (dashed lines) were recorded in air-saturated buffer. The spectra of reduced chlorosomes (solid lines) were recorded after treatment with 25 mM sodium dithionite and incubation in the dark for 1 h. Adapted from [24] for comparison with Fig. 4.

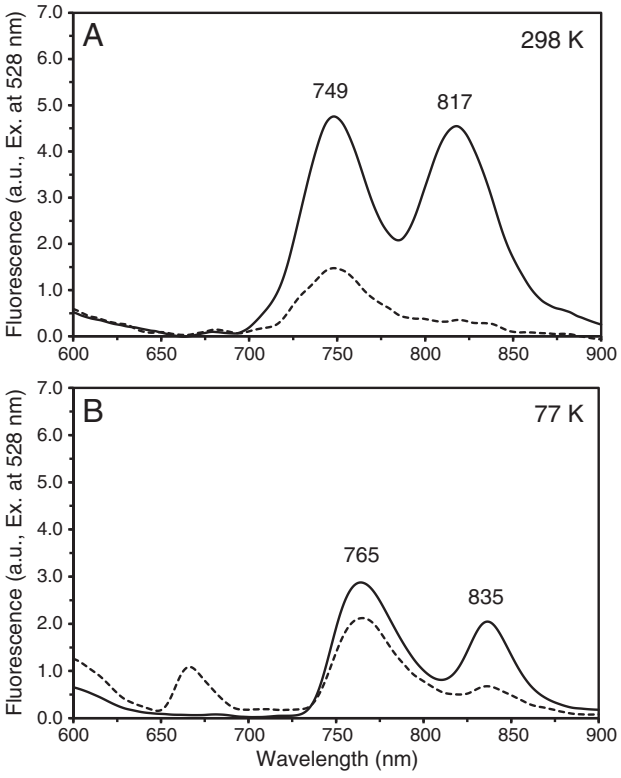

Fig. 4. Fluorescence emission spectra for BChl *e*-containing chlorosomes at room temperature (A) and 77 K (B). The excitation wavelength was into the longer-wavelength Soret component at 528 nm for each. Spectra of oxidized chlorosomes (dashed lines) were recorded in air-saturated buffer. The spectra of reduced chlorosomes (solid lines) were recorded after treatment with 25 mM sodium dithionite and incubation in the dark for 1 h.

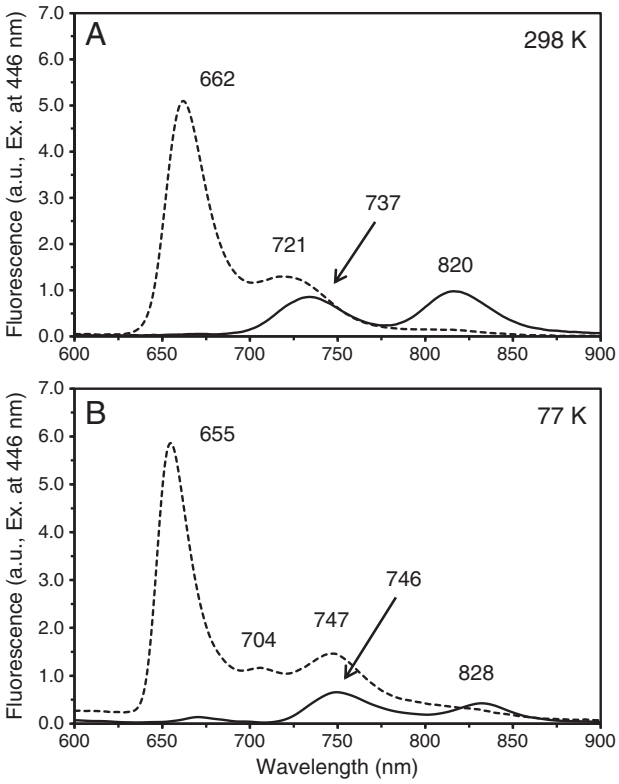

Fig. 5. Fluorescence emission spectra for BChl *f*-containing chlorosomes at room temperature (A) and 77 K (B). The excitation wavelength was into the shorter-wavelength Soret component at 446 nm for each. Spectra of oxidized chlorosomes (dashed lines) were recorded in air-saturated buffer. The spectra of reduced chlorosomes (solid lines) were recorded after treatment with 25 mM sodium dithionite and incubation in the dark for 1 h. Adapted from [24] for comparison with Fig. 6.

due in part to a perturbation (which confers stability) caused by the change of environment polarizability (liquid to glass) at low temperatures. Because the Q_y transition is a collection of excitonic transitions (as evidenced in Fig. 8, described in detail in Section 3.3), this shift is also attributed to a redistribution of the excitonic population probability to lower energies at lower temperatures. The scaling factors introduced Section 2.2 changed the spectra minimally; the ratio of 1-*T* spectral ordinances varied between 0.90 and 1.01.

Figs. 5 and 6 show the corresponding fluorescence emission spectra that result from excitation of the two Soret band components of chlorosomes containing BChl *f*. A different trend is observed here. The fluorescence emission resulting from excitation of the shorter wavelength Soret component (Fig. 5, centered at 446 nm) in air-oxidized conditions contains significantly higher amplitude of fluorescence from BChl *f* monomers. It should also be noted that any BChl *f* monomers that are present will also absorb at this excitation wavelength, but according to the absorption spectrum shown in Fig. 1, this should be minimal. The emission contribution from the BChl *f* monomers is much higher than expected, which possibly indicates that there is a different energy-level mixing in these chlorosomes than would be expected from the calculations in [30]. In contrast, the fluorescence emission from the longer wavelength Soret component (Fig. 6 centered at 508 nm) corresponds nearly identically in pattern to the counterpart for BChl *e*. It should also be noted that for excitation in the shorter wavelength Soret band at low temperatures (Fig. 5B), the fluorescence emission from the BChl *f* oligomers is split into two distinct components centered at 704 nm and 747 nm [24]. The component emitting at 704 nm corresponds to a low-energy vibronic level of the BChl *f* monomer, and the component emitting at 747 nm corresponds to the fluorescence emission from BChl *f* oligomers. All preparations of chlorosomes containing BChl *f* had lower fluorescence emission amplitudes from the BChl *a*-, CsmA-containing baseplate than chlorosomes containing BChl *e* having the same absorbance in the Q_y band.

3.2. Fluorescence excitation spectra and efficiency estimates

Fig. 7 shows the fluorescence excitation spectra of intact photosynthetic membranes of WT *Cba. limnaeum* (containing BChl *e*, Fig. 7A) and of the *bchU* mutant (containing BChl *f*, Fig. 7B) overlaid with the corresponding 1-*T* spectra. By normalizing the amplitude of the two spectra at the excitation maximum of the lowest-energy acceptor molecule, the energy transfer efficiency can be estimated. It is assumed here that energy transfer efficiency from the chlorosome baseplate to the acceptors in the membrane is the same between the two types of chlorosomes, and that it is close to 100%. Under this assumption and the conditions employed, Fig. 7A shows that BChl *e* oligomers are able to transfer energy with an overall efficiency of ~65%. In contrast, BChl *f* oligomers are only able to transfer energy with an efficiency of ~39% (Fig. 7B).

3.3. Circular dichroism spectroscopy

Fig. 8 shows the CD spectra (Fig. 8A) of chlorosomes containing BChl *e* and BChl *f*, along with their second derivatives (Fig. 8B). The spectra in Fig. 8A appear to be consistent with those for molecular species exhibiting exciton-coupled energy transfer processes, which indicate that the main light-harvesting pigments in each type of chlorosome are strongly coupled. The second derivatives in Fig. 8B confirm that the CD spectra in Fig. 8A are centered upon their respective absorption maxima. The shapes of the second derivatives further indicate that the CD spectra suggest the presence of only a single spectral component in each type of chlorosome.

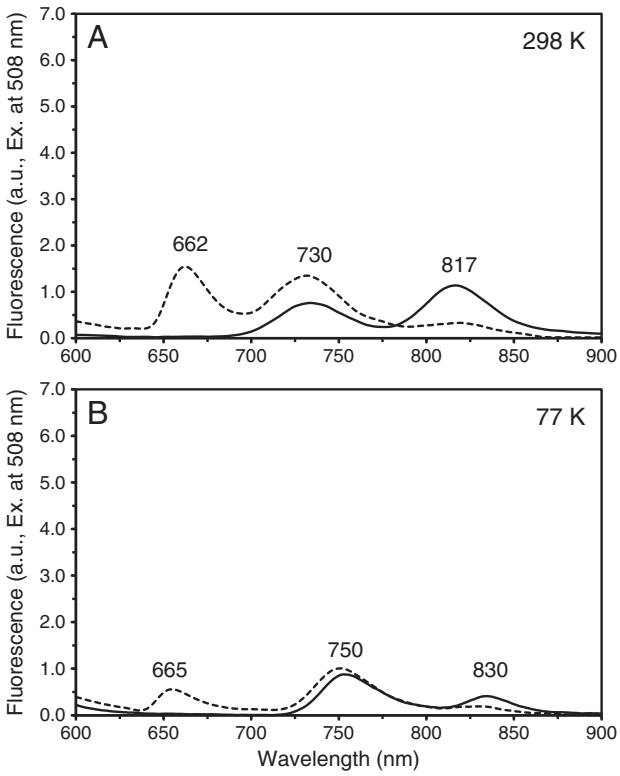

Fig. 6. Fluorescence emission spectra for BChl *f*-containing chlorosomes at room temperature (A) and 77 K (B). The excitation wavelength was into the longer-wavelength Soret component at 508 nm for each. Spectra of oxidized chlorosomes (dashed lines) were recorded in air-saturated buffer. The spectra of reduced chlorosomes (solid lines) were recorded after treatment with 25 mM sodium dithionite and incubation in the dark for 1 h.

3.4. Quantum yield and fluorescence lifetime measurements of isolated BChl *f*

Fig. 9 shows the results of a determination of quantum yield for BChl *f* that was determined by comparison with a previously characterized BChl *c* standard [27]. The fluorescence spectra of the concentration series of BChl *c* and BChl *f* are shown in Fig. 9A. By integrating each spectrum and converting these data to a plot of integrated fluorescence vs. absorbance at the excitation wavelength for each member of the series, an *x*–*y* scatter plot can be constructed. A linear regression of each data set yields a slope (gradient) that can be used in Eq. (1). The correction introduced in Eq. (2) is quite small; the ratio of the two 1-*T* spectral ordinances was 0.99. Upon inserting the appropriate values into Eq. (2), the fluorescence quantum yield of BChl *f* was found to be 0.13, a value about 50% less than that of BChl *c*.

The time-resolved fluorescence data derived from the streak camera measurements are shown in Fig. 10A. This two-dimensional image was used to construct the fluorescence emission spectrum (Fig. 10B) and fluorescence kinetics (Fig. 10C). After applying a single exponential decay fit to the fluorescence kinetic trace, the singlet excited-state lifetime for BChl *f* in pyridine was determined to be 3.4 ns. This lifetime is comparable to the previously determined singlet excited-state lifetime of 2.9 ns for BChl *e* in pyridine and significantly less than the lifetimes observed for BChl *c* and *d* (6.7 and 6.3 ns, respectively) [31].

3.5. Energy transfer calculations using FRET theory

Table 1 shows the Gaussian simulation parameters for the fluorescence emission of dithionite-reduced BChl *e* and *f* chlorosomes from this study, compared with those from BChl *c* and *d* chlorosomes from another study [29]. The data from Table 1 indicate that the peak widths of fluorescence components are very similar between chlorosomes of different pigment compositions. Even when the main light-harvesting pigment changed from BChl *c* to BChl *d*, BChl *e*, or BChl *f*, the

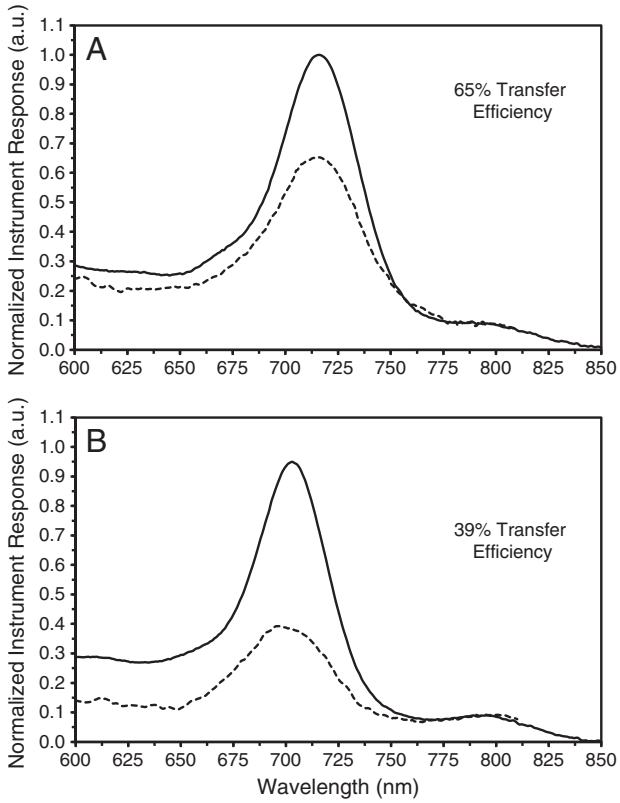

Fig. 7. Excitation spectra (dashed lines) overlaid with the respective 1-*T* spectra (solid lines) of BChl *e*-containing (A) and BChl *f*-containing (B) chlorosomes.

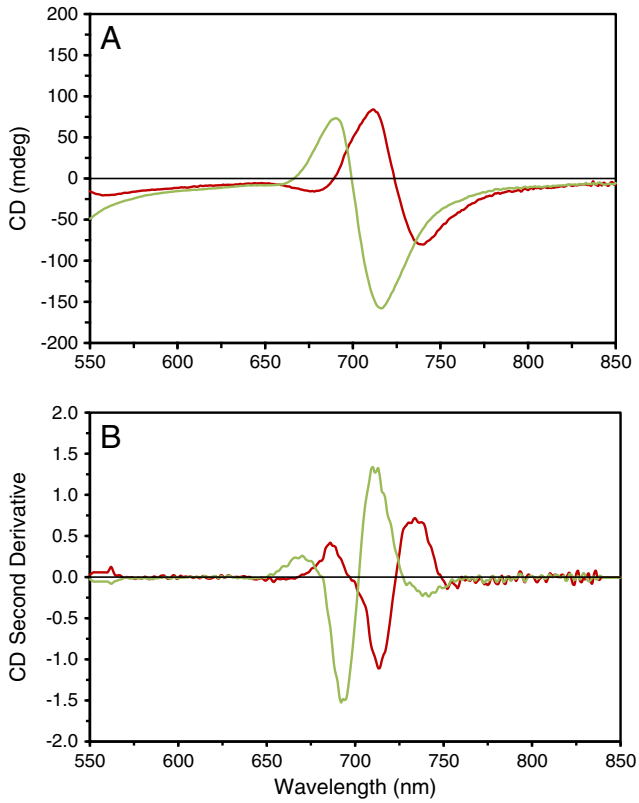

Fig. 8. Circular dichroism spectra (A) and their second derivatives (B) of BChl *e*-containing (red line) and BChl *f*-containing (green line) chlorosomes.

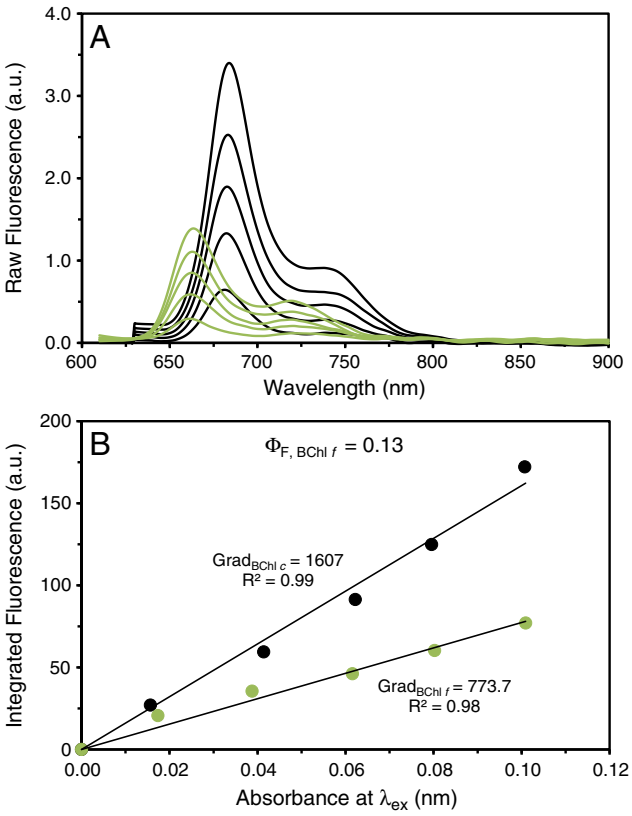

Fig. 9. The corrected fluorescence emission for a concentration series of BChl *c* (black lines) and BChl *f* (green lines) (A), along with the linear correlation of integrated fluorescence vs. absorbance for determination of the fluorescence quantum yield of monomeric BChl *f* (B). BChl *c* was used the known quantum yield reference. The solvent for all measurements was degassed pyridine.

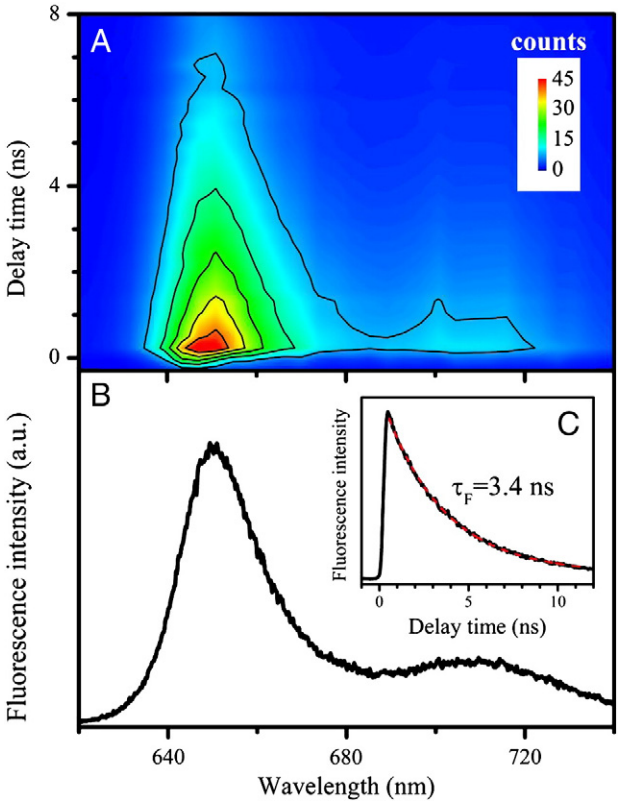

Fig. 10. (A) Time-resolved fluorescence profile of BChl *f* taken in pyridine at room temperature. The y-axis represents fluorescence intensity and is expressed in photon counts (see legend); (B) fluorescence spectrum obtained by summation of the time-resolved fluorescence spectra taken in time range between 1 and 4 ns; (C) representative kinetic trace of fluorescence decay measured at the maximum of the fluorescence band. The dashed red line represents single exponential decay fit that determined the fluorescence lifetime of 3.4 ns.

fluorescence emission from the BChl *a*-containing CsmA baseplate had essentially the same maximal wavelength.

As mentioned in Section 2.7, absorption of the BChl *a*-containing baseplate component can be estimated as a Gaussian centered at 789.1 nm with a width of 48.5 nm [29]. Thus, a direct comparison of the overlap between BChl *e* and the baseplate and BChl *f* and the baseplate can be made. This comparison is depicted in Fig. 11. This analysis shows that the calculated mathematical overlap area for BChl *f* oligomers and the baseplate is 47% smaller than that for BChl *e* oligomers and the baseplate. The basic mathematical overlap area, however, cannot be used in a FRET theory treatment of energy transfer from major BChl to the baseplate in the system. Rather, the *J* function described in Eq. (5) must be used. Table 2 summarizes the relevant overlap factors determined in this study. Noting from Fig. 7A that the efficiency of BChl *e*-BChl *a* transfer in BChl *e* chlorosomes is ~65%, the FRET efficiency of BChl *f*-BChl *a* transfer in BChl *f* can be calculated to be 41%. This calculation is in excellent agreement with the experimental determination (39%) as described in Section 3.2 and as shown in Fig. 7B.

4. Discussion

This study sought to further understand the similarities and differences between chlorosomes containing the naturally occurring pigment, BChl *e* and chlorosomes from a *bchU* mutant of *Cba. limnaeum* that contain BChl *f*. It has previously been shown that the *Cba. limnaeum* mutant producing BChl *f* instead of BChl *e* is viable, although its doubling time is about 40% slower under low irradiance conditions [24]. Sufficient data now exists to explain this phenotypic difference from a biophysical perspective.

Although variations in the relative contribution of fluorescence from oligomer BChl *e*/*f* vs. baseplate BChl *a* based on excitation wavelength can be seen, fluorescence emission spectra show that chlorosomes containing BChl *f* consistently display a lower fluorescence emission from the CsmA baseplate than chlorosomes containing BChl *e*. These variations may indicate that slightly different oligomeric structural types of BChl exist between these chlorosomes. Perhaps a better indication of structural difference is the narrower absorption bandwidth of the BChl *f* aggregates in the mutant chlorosomes vs. the BChl *e* aggregates in the WT. This lessened inhomogeneous broadening likely means that the BChl oligomerization regime is more regular throughout the entirety of the chlorosome in the *bchU* mutant than in the WT.

Additionally, after air oxidation, chlorosomes containing BChl *f* also consistently showed a higher fluorescence emission from BChl *f*

Table 1
Fitting parameters for Gaussian simulations of fluorescence emission spectra of fully reduced, isolated chlorosomes containing BChl *c*, *d*, *e*, or *f*.

	BChl *c*[a]	BChl *d*[a]	BChl *e*[b]	BChl *f*[b]
Main Pigment Gaussian:				
Amplitude	0.972	0.998	0.960	0.951
Wavelength (nm)	775.7	759.8	744.1	730.2
Width (nm)	44.1	43.8	36.6	36.1
Baseplate Gaussian:				
Amplitude	0.304	1.363	0.597	1.065
Wavelength (nm)	810.1	807.3	812.5	813.3
Width (nm)	29.3	30.1	44.4	40.4

Each spectrum was normalized to a maximum of 1.0 for the BChl *c*, *d*, *e*, or *f* emission peak.
[a] From Causgrove et. al., 1992.
[b] From this work.

monomers. This indicates one way in which energy transfer in chlorosomes containing BChl *f* is inhibited in comparison to the BChl *e* system. This result is strongly supported by the fluorescence excitation experiments, which are a more direct measurement of energy transfer events. As mentioned in Section 3.2, Fig. 7 shows that the chlorosomes containing BChl *f* transfer energy nearly 40% less efficiently to the remainder of the photosynthetic apparatus than chlorosomes containing BChl *e*.

With only these results in hand, it is reasonable to ask whether this efficiency decrease is due to less optimal absorption properties of the BChl *f* molecule, substantial differences in its oligomerization and organization, a decreased spectral overlap with the BChl *a* acceptor in the baseplate, or a combination of all three. The BChl *e* and BChl *f* molecules only differ structurally by a single methyl group at the C-20 position, but it has long been known that even minor differences in the substituents of chlorin or bacteriochlorin rings can appreciably change their spectroscopic and structural properties, possibly by puckering of the chlorin ring [32,33]. Examples include the Chl *a* and Chl *b* pairs, as well as the BChl *a* and BChl *b* pairs [19]. The quantum yield and lifetime measurements, circular dichroism spectroscopy, and FRET theory calculations performed here serve to address this question.

Experiments with monomeric BChl *f* in pyridine show that its fluorescence quantum yield is 0.13. Although this is a 50% decrease from that of BChl *c*, this quantum yield is not substantially different from the values for other *Chlorobium* BChls. In contrast, the fluorescence lifetime of BChl *f* was found to be slightly longer than that of BChl *e*, which further emphasizes their similar spectroscopic properties. However, considering that the majority of the BChls in chlorosomes should be organized in oligomers that are strongly coupled excitonically (as evidenced by the absorption spectra in Fig. 1 and the CD spectra in Fig. 8), small differences in the fluorescence quantum yield or lifetimes of monomers should not, by themselves, be responsible for the major differences in energy transfer observed for chlorosomes and cells of the *bchU* mutant.

The circular dichroism results show similarity in the excitonic coupling of the pigment oligomeric structures in chlorosomes containing BChl *e* and BChl *f*. Both types of chlorosomes show strong excitonic coupling, which leads to long-range energy transfer across the oligomeric structures and ultimately facilitates energy transfer to the BChl *a* associated with the CsmA in the baseplate. While the time-dependent rates of this energy transfer will be explored in later studies, it can be concluded from the findings in this study that chlorosomes containing BChl *f* are functionally quite similar to their counterparts containing BChl *c*, *d*, or *e*. Therefore, we conclude that monomeric BChl *f* is similar to these other three BChls and that the differences observed for chlorosomes containing BChl *f* are not the result of extensive differences in oligomeric excitonic coupling of the BChls or to fundamental differences in the biophysical properties of BChl *f*.

The FRET analysis of the two systems, however, identified a major difference and the possible source of the energy transfer inefficiency. The observed 47% decrease in overlap for the donor and acceptor pair when replacing BChl *e* with *f* corresponds to a 40% decrease in overall FRET efficiency, assuming that the relative concentrations of donor and acceptor are the same between the two chlorosome systems. Because our estimates of differences in energy transfer efficiency from the FRET analysis match quite well with the estimate from fluorescence excitation, we conclude that the observed decreased efficiency in energy transfer in chlorosomes containing BChl *f* is primarily due to the decreased spectral overlap between BChl *f* oligomeric donors and BChl *a* acceptors. Considering the otherwise high degree of similarity observed for chlorosomes containing BChl *e* or BChl *f*, this large decrease in the spectral overlap is currently the only identified parameter that can explain the very large decrease in energy transfer efficiency reported here. This is manifested as a two-fold slower growth rate at low light intensity [21], which would not allow organisms producing BChl *f* to compete favorably in the same niches with organisms synthesizing BChl *e*.

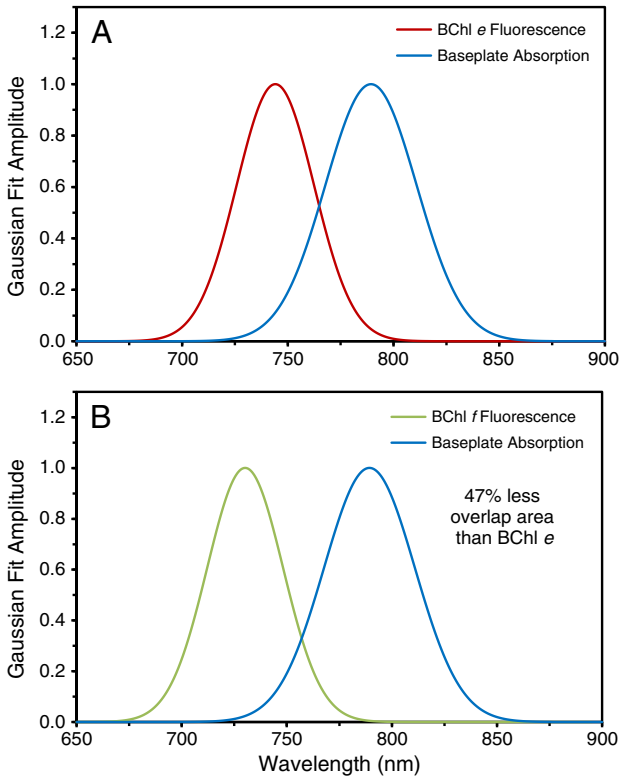

Fig. 11. Gaussian simulations and spectral overlap comparison of BChl *e*-containing (A) and BChl *f*-containing (B) chlorosomes.

5. Conclusions

This study reports the results from a detailed spectroscopic analysis of chlorosomes containing BChl *f* from a *bchU* mutant of the GSB *Cba. limnaeum*. The slow growth rate of this mutant at low irradiance can be attributed in part to decreased efficiency of energy transfer within the chlorosomes from BChl oligomer to baseplate. This decreased efficiency, in turn, can be attributed almost exclusively to a decreased spectral overlap between the oligomeric BChl *f* donors and BChl *a* acceptors associated with the chlorosome baseplate, as compared to the oligomeric BChl *e* donors and the same BChl *a* acceptor in WT chlorosomes. Time-resolved spectroscopic studies, as well as high-resolution microscopy, will complement these findings and may possibly elucidate additional causes for the decreased efficiency of energy transfer (i.e., slight variations in BChl oligomer structures). Further experiments must also be done to explain the unusually high fluorescence amplitude from monomeric BChl *f* that occurs within chlorosomes containing BChl *f* after exposure to oxygen. There may be an unresolved structural

Table 2
Spectral overlap factors for energy transfer from chlorosomes containing BChl *e* and *f*.

	BChl *e*	BChl *f*
Overlap area between main pigment and BChl *a* relative to BChl *e* from basic spectral integration	1.00	0.53
FRET theory *J* factor	3.32×10^{12}	1.25×10^{12}
Estimated FRET efficiency from main pigment to BChl *a* using Eq. (6)	0.65	0.41

Overlap factors were determined from the emission parameters of Table 1 and a Gaussian for the BChl *a* absorption in the baseplate centered at 789.1 nm with a width of 48.5 nm. The baseplate Gaussian parameters are taken from Causgrove et. al., 1992. The efficiency value of 0.65 for BChl *e* is an estimate taken from Fig. 7.

rearrangement or mixing of absorption bands occurring in the Soret region that could explain this observation.

Although they have thus far eluded discovery, there is no fundamental reason why organisms containing BChl *f* could not be found in nature. The *bchU* mutation is not lethal, and the associated growth defects for cells producing BChl *f* are similar in magnitude to those observed for organisms that synthesize BChl *d* [23]. However, any green sulfur bacterium producing BChl *f* would probably require a high irradiance niche; otherwise it would have to compete with organisms producing BChl *e* that would probably coexist in the same environments. Such an organism would also probably receive light that would be filtered by organisms containing Chl *a*, Chl *b*, and possibly Chl *d*. Lastly, the niche would need to be anoxic and contain either thiosulfate or sulfide, or both. High irradiance environments devoid of these filtering effects and atmospheric oxygen are probably rare, and the potential competitors are numerous and diverse. An example of such a niche could be a sun-exposed, anoxic, saline lagoon devoid of plant or algal life, such as those found in land-locked desert salt lakes. A certainty is that organisms potentially producing BChl *f* have had a very long time, perhaps >2 billion years, to adapt to such niches. So, it remains possible that organisms producing BChl *f* may be found in nature.

Conflict of interest statement

The authors declare that the research was conducted in the absence of any commercial or financial relationships that could be construed as a potential conflict of interest.

Acknowledgements

The purification and spectroscopy studies were supported by The Photosynthetic Antenna Research Center, an Energy Frontier Research Center funded by the U.S. Department of Energy, Office of Science, Office of Basic Energy Sciences under award DE-SC0001035 to R.E.B. Work involving genetic manipulation and microbial culturing was supported by the U.S. Department of Energy, under grant DE-FG02-94ER20137 to D.A.B.

References

[1] R.E. Blankenship, K. Matsuura, Antenna complexes from green photosynthetic bacteria, in: B.R. Green, W.W. Parson (Eds.), Advances in Photosynthesis and Respiration, Light Harvesting Antennas in Photosynthesis, vol. 13, Kluwer, 2003, pp. 195–217.
[2] G.T. Oostergetel, H. van Amerongen, E.J. Boekema, The chlorosome: a prototype for efficient light harvesting in photosynthesis, Photosynth. Res. 104 (2010) 245–255.
[3] D.A. Bryant, Z. Liu, T. Li, F. Zhao, A.M. Garcia Costas, C.G. Klatt, D.M. Ward, Comparative and functional genomics of anoxygenic green bacteria from the Taxa *Chlorobi*, *Chloroflexi*, and *Acidobacteria*, in: R. Burnap, W. Vermaas (Eds.), Functional Genomics and Evolution of Photosynthetic Systems, Springer Netherlands, Dordrecht, 2012, pp. 47–102.
[4] A.K. Manske, J. Glaeser, M.M.M. Kuypers, Physiology and phylogeny of green sulfur bacteria forming a monospecific phototrophic assemblage at a depth of 100 M, Appl. Environ. Microbiol. 71 (2005) 8049–8060.
[5] G.A. Montaño, B.P. Bowen, J.T. LaBelle, N.W. Woodbury, V.B. Pizziconi, R.E. Blankenship, Characterization of *Chlorobium tepidum* chlorosomes: a calculation of bacteriochlorophyll *c* per chlorosome and oligomer modeling, Biophys. J. 85 (2003) 2560–2565.
[6] S. Ganapathy, G.T. Oostergetel, P.K. Wawrzyniak, M. Reus, A. Gomez Maqueo Chew, F. Buda, E.J. Boekema, D.A. Bryant, A.R. Holzwarth, H.J.M. de Groot, Alternating syn-anti bacteriochlorophylls form concentric helical nanotubes in chlorosomes, PNAS 106 (2009) 8525–8530.
[7] S. Ganapathy, G.T. Oostergetel, M. Reus, Y. Tsukatani, A. Gomez Maqueo Chew, F. Buda, D.A. Bryant, A.R. Holzwarth, H.J.M. de Groot, Structural variability in wild-type and *bchQ bchR* Mutant chlorosomes of the green sulfur bacterium *Chlorobaculum tepidum*, Biochemistry 51 (2012) 4488–4498.
[8] A.M. Garcia Costas, Y. Tsukatani, S.P. Romberger, G.T. Oostergetel, E.J. Boekema, J.H. Golbeck, D.A. Bryant, Ultrastructural analysis and identification of envelope proteins of "*Candidatus* Chloracidobacterium thermophilum" chlorosomes, J. Bacteriol. 193 (2011) 6701–6711.
[9] T.S. Balaban, A.R. Holzwarth, K. Schaffner, G.J. Boender, H.J. de Groot, CP-MAS 13C-NMR dipolar correlation spectroscopy of 13C-enriched chlorosomes and isolated bacteriochlorophyll *c* aggregates of *Chlorobium tepidum*: the self-organization of pigments is the main structural feature of chlorosomes, Biochemistry 34 (1995) 15259–15266.
[10] V.I. Prokhorenko, D.B. Steensgaard, A.R. Holzwarth, Exciton theory for supramolecular chlorosomal aggregates: 1 aggregate size dependence of the linear spectra, Biophys. J. 85 (2003) 3173–3186.
[11] R. Frese, U. Oberheide, I.V. Stokkum, R.V. Grondelle, M. Foidl, H.V. Amerongen, The organization of bacteriochlorophyll *c* in chlorosomes from *Chloroflexus aurantiacus* and the structural role of carotenoids and protein: an absorption, linear dichroism, circular dichroism and Stark spectroscopy study, Photosynth. Res. (1997) 115–126.
[12] N.-U. Frigaard, S. Takaichi, M. Hirota, K. Shimada, K. Matsuura, Quinones in chlorosomes of green sulfur bacteria and their role in the redox-dependent fluorescence studied in chlorosome-like bacteriochlorophyll *c* aggregates, Arch. Microbiol. 167 (1997) 343–349.
[13] N.-U. Frigaard, J.A. Maresca, C.E. Yunker, A.D. Jones, D.A. Bryant, Genetic Manipulation of carotenoid biosynthesis in the green sulfur bacterium *Chlorobium tepidum*, J. Bacteriol. 186 (2004) 5210–5220.
[14] A. Gomez Maqueo Chew, N.-U. Frigaard, D.A. Bryant, Bacteriochlorophyllide c C-8(2) and C-12(1) methyltransferases are essential for adaptation to low light in *Chlorobaculum tepidum*, J. Bacteriol. 189 (2007) 6176–6184.
[15] J.A. Maresca, J.E. Graham, D.A. Bryant, The biochemical basis for structural diversity in the carotenoids of chlorophototrophic bacteria, Photosynth. Res. 97 (2008) 121–140.
[16] G.A. Montaño, H.-M. Wu, S. Lin, D.C. Brune, R.E. Blankenship, Isolation and characterization of the B798 light-harvesting baseplate from the chlorosomes of *Chloroflexus aurantiacus*, Biochemistry 42 (2003) 10246–10251.
[17] J. Pšenčík, A.M. Collins, L. Liljeroos, M. Torkkeli, P. Laurinmäki, H.M. Ansink, T.P. Ikonen, R.E. Serimaa, R.E. Blankenship, R. Tuma, S.J. Butcher, Structure of chlorosomes from the green filamentous bacterium *Chloroflexus aurantiacus*, J. Bacteriol. 191 (2009) 6701–6708.
[18] R.Y.-C. Huang, J. Wen, R.E. Blankenship, M.L. Gross, Hydrogen-deuterium exchange mass spectrometry reveals the interaction of Fenna-Matthews-Olson protein and chlorosome CsmA protein, Biochemistry 51 (2012) 187–193.
[19] R.E. Blankenship, Molecular Mechanisms of Photosynthesis, 1st ed. Blackwell Science, Malden, MA, 2002.
[20] R.E. Blankenship, Identification of a key step in the biosynthetic pathway of bacteriochlorophyll *c* and its implications for other known and unknown green sulfur bacteria, J. Bacteriol. 186 (2004) 5187–5188.
[21] H. Tamiaki, J. Komada, M. Kunieda, K. Fukai, T. Yoshitomi, J. Harada, T. Mizoguchi, In vitro synthesis and characterization of bacteriochlorophyll-f and its absence in bacteriochlorophyll-e producing organisms, Photosynth. Res. 107 (2011) 133–138.
[22] N.-U. Frigaard, D.A. Bryant, Chromosomal gene inactivation in the green sulfur bacterium *Chlorobium tepidum* by natural transformation chromosomal gene inactivation in the green sulfur bacterium *Chlorobium tepidum* by natural transformation, Appl. Environ. Microbiol. 67 (2001) 2538–2544.
[23] J.A. Maresca, A. Gomez Maqueo Chew, M.R. Ponsatí, N. Frigaard, J.G. Ormerod, D.A. Bryant, The bchU gene of *Chlorobium tepidum* encodes the C-20 methyltransferase in bacteriochlorophyll *c* biosynthesis, J. Bacteriol. 186 (2004) 2558–2566.
[24] K. Vogl, M. Tank, G.S. Orf, R.E. Blankenship, D.A. Bryant, Bacteriochlorophyll f: properties of chlorosomes containing the "forbidden chlorophyll", Front. Microbiol. 3 (2012) 1–12.
[25] J. Harada, T. Mizoguchi, Y. Tsukatani, M. Noguchi, H. Tamiaki, A seventh bacterial chlorophyll driving a large light-harvesting antenna, Sci. Rep. 2 (2012) 671.
[26] P.D. Gerola, J.M. Olson, A new bacteriochlorophyll a-protein complex associated with chlorosomes of green sulfur bacteria, Biochim. Biophys. Acta 848 (1986) 69–76.
[27] D. Brune, R. Blankenship, G. Seely, Fluorescence quantum yields and lifetimes for bacteriochlorophyll c, Photochem. Photobiol. 47 (1988) 759–763.
[28] A.T.R. Williams, S.A. Winfield, J.N. Miller, Relative fluorescence quantum yields using a computer-controlled luminescence spectrometer, Analyst 108 (1983) 1067–1071.
[29] T.P. Causgrove, D.C. Brune, R.E. Blankenship, Förster energy transfer in chlorosomes of green photosynthetic bacteria, J. Photochem. Photobiol. B Biol. 15 (1992) 171–179.
[30] Y. Shibata, S. Tateishi, S. Nakabayashi, S. Itoh, H. Tamiaki, Intensity borrowing via excitonic couplings among soret and Q(y) transitions of bacteriochlorophylls in the pigment aggregates of chlorosomes, the light-harvesting antennae of green sulfur bacteria, Biochemistry 49 (2010) 7504–7515.
[31] D.M. Niedzwiedzki, R.E. Blankenship, Singlet and triplet excited state properties of natural chlorophylls and bacteriochlorophylls, Photosynth. Res. 106 (2010) 227–238.
[32] A. Struck, E. Cmiel, I. Katheder, W. Schafer, H. Scheer, Bacteriochlorophylls modified at position C-3: long range intramolecular interaction with position C-132, Biochim. Biophys. Acta 1101 (1992) 321–328.
[33] M. Senge, N.W. Smith, K.M. Smith, Structure and conformation of photosynthetic pigments and related compounds 5′ structural investigation of nickel(II) bacteriopetroporphyrins related to the bacteriochlorophylls c and d: evidence for localized conformational distortion in the c-series, Inorg. Chem. 32 (1993) 1259–1265.